Supplement of The Cryosphere, 18, 3825–3839, 2024
https://doi.org/10.5194/tc-18-3825-2024-supplement

The Cryosphere Open Access EGU

Supplement of

The role of atmospheric conditions in the Antarctic sea ice extent summer minima

Bianca Mezzina et al.

Correspondence to: Bianca Mezzina (bianca.mezzina@uclouvain.be)

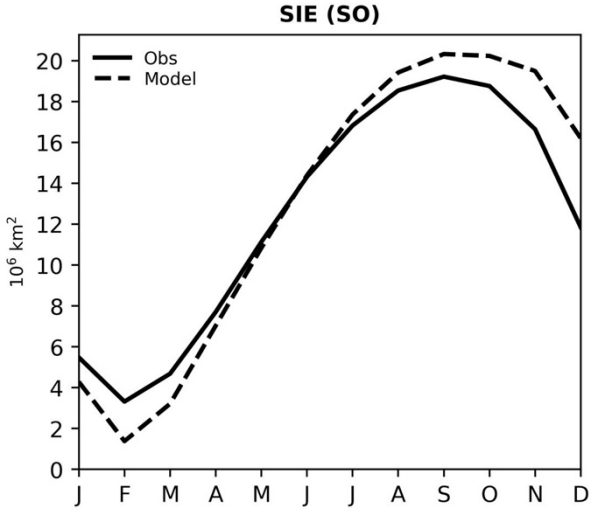

Figure S1: Seasonal cycle of the total Antarctic SIE in the observations (solid line) and in the model (dashed line).

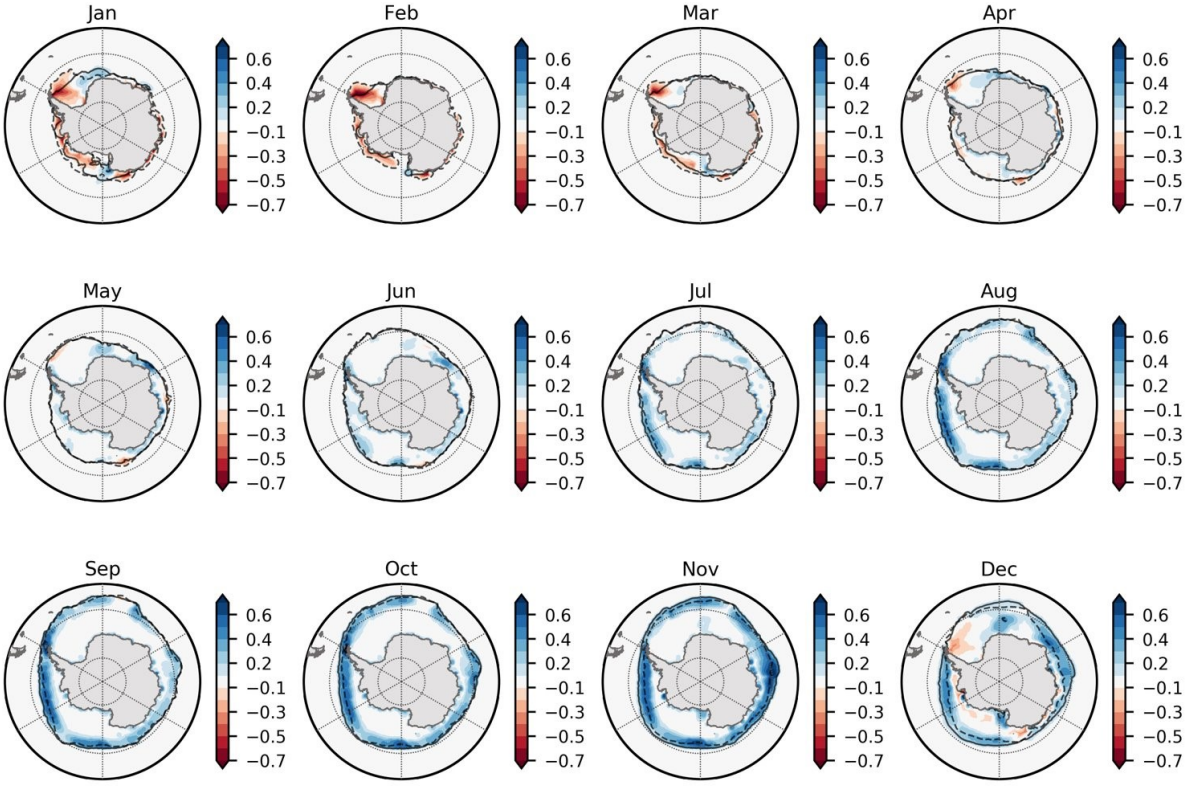

Figure S2: Differences in the monthly SIC climatology between the model and the observations.

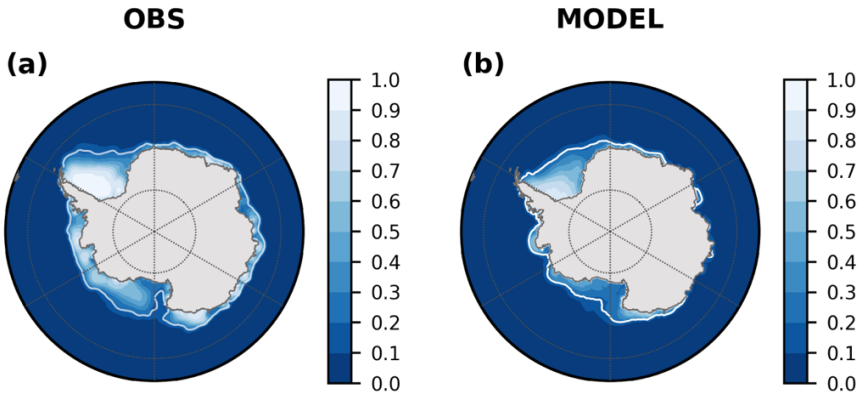

Figure S3: JFM climatology of the SIC in the (a) observations and (b) model. The solid line indicates SIC=0.15.

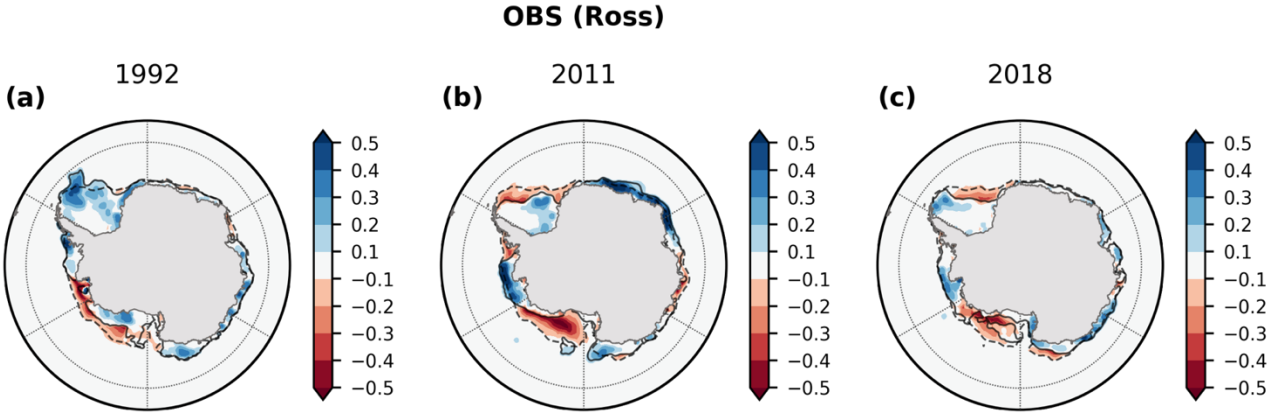

Figure S4: Shading: observed SIC anomalies in JFM in the years with SIE minima in the Ross Sea. Contours: sea ice edge (SIC=0.15) in the respective years (solid line) and in the climatology (dashed line).

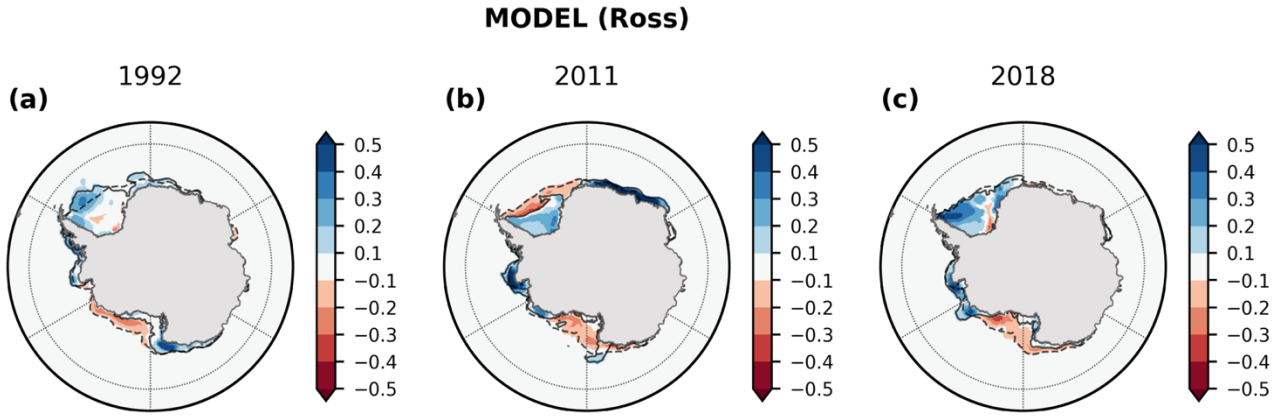

Figure S5: Same as Fig. S2, but for the model.

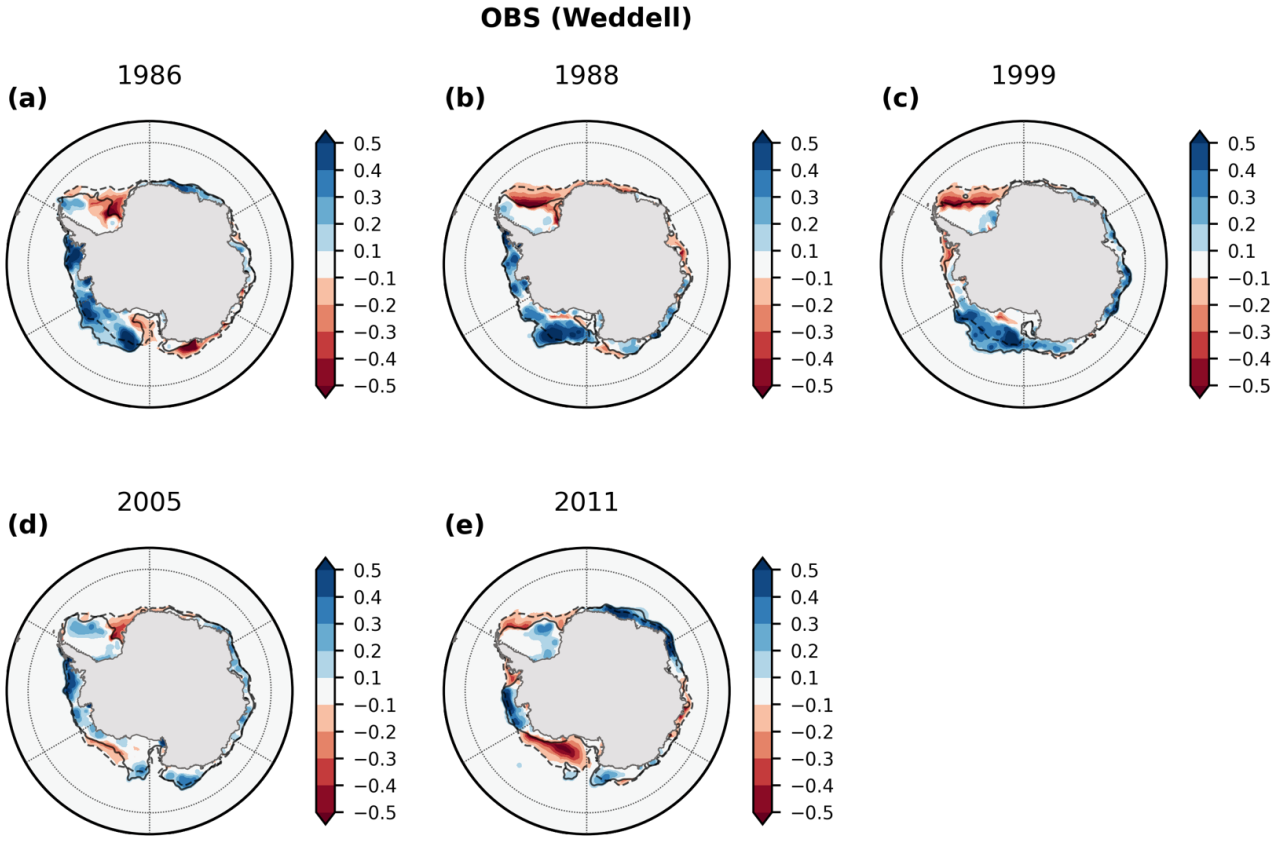

Figure S6: Shading: observed SIC anomalies in JFM during the years with SIE minima in the Weddell Sea. Contours: sea ice edge (SIC=0.15) in the respective years (solid line) and in the climatology (dashed line).

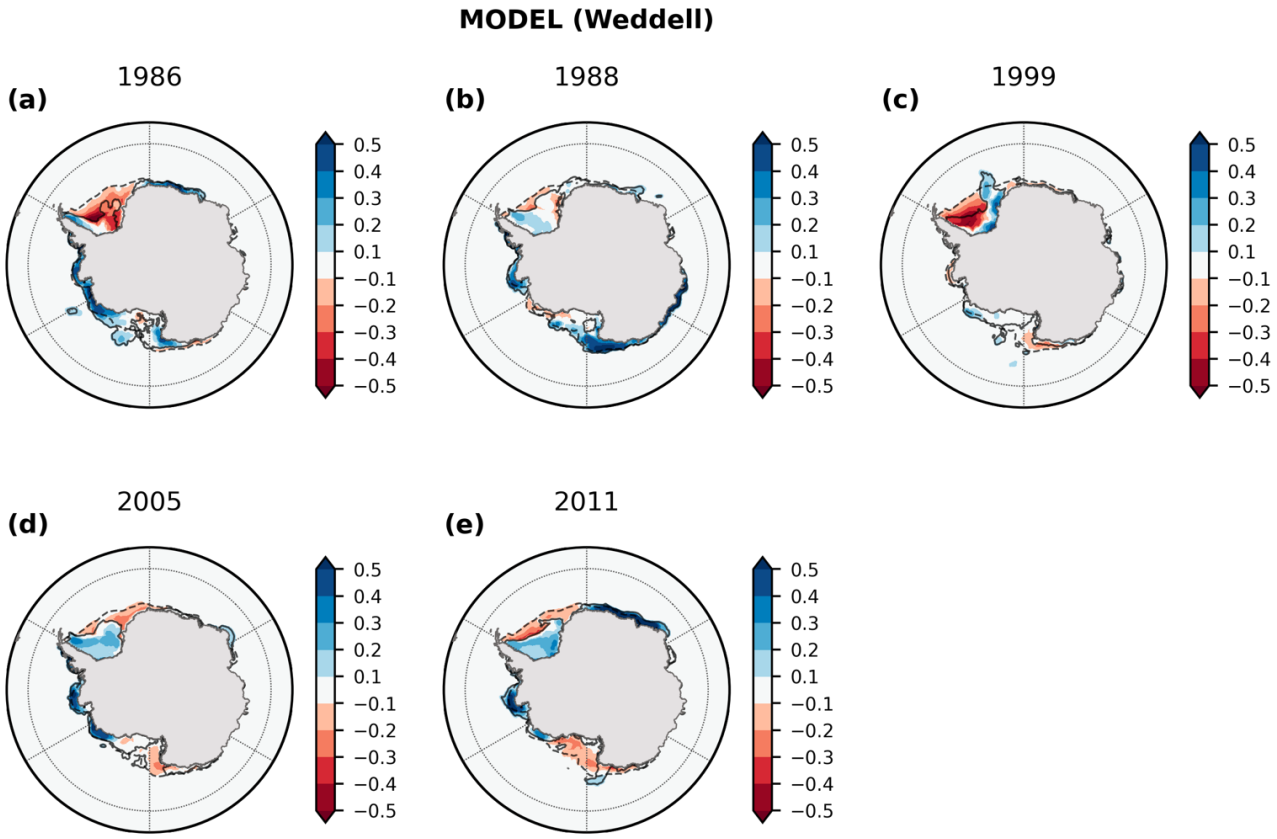

Figure S7: Same as Fig. S4, but for the model.

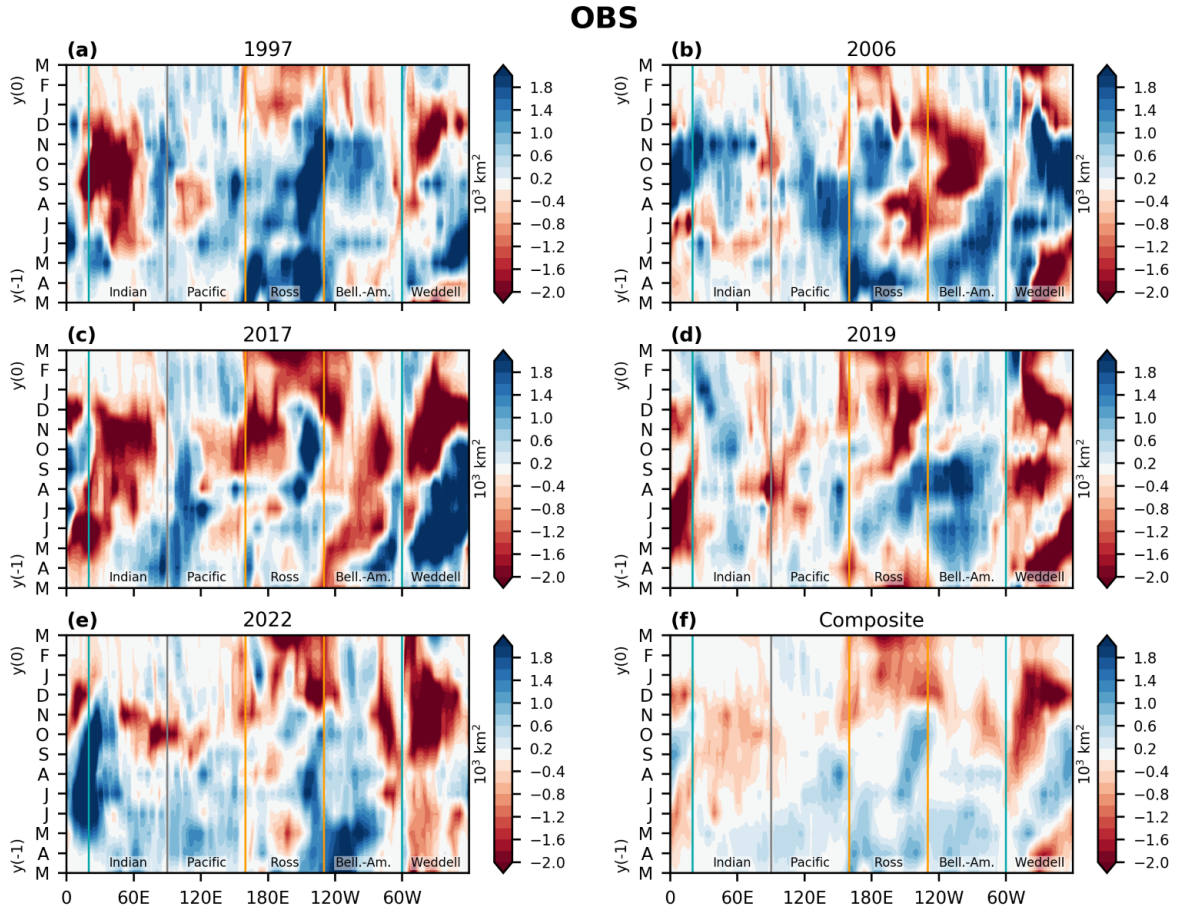

Figure S8: Time-longitude sea ice area anomalies for the five total minima and their composite, in the observations. The vertical axis displays time, starting from one year before the minimum at the bottom (e.g. March 1996 in the first panel) up to the event itself (e.g. March 1997) at the top.

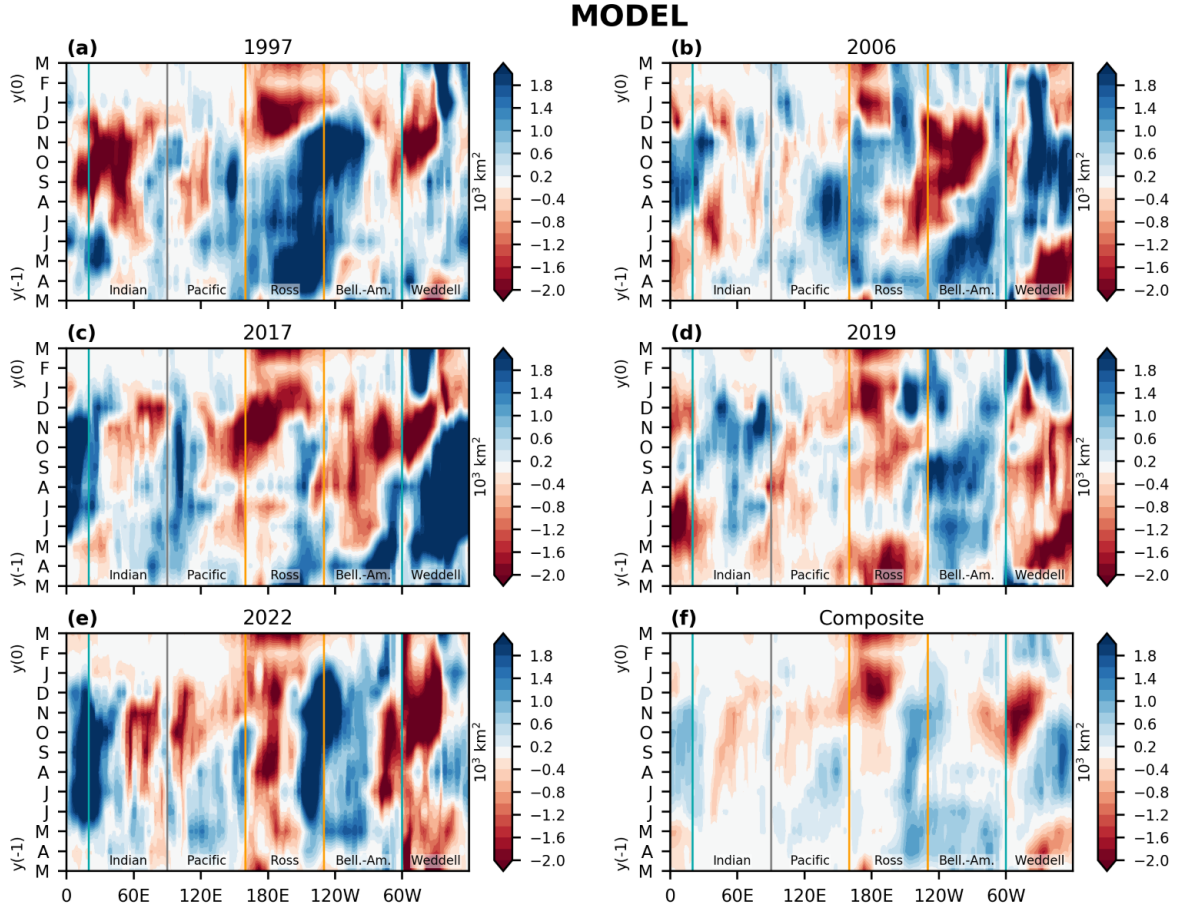

Figure S9: Time-longitude sea ice area anomalies for the five total minima and their composite, in the model. The vertical axis displays time, starting from one year before the minimum at the bottom (e.g. March 1996 in the first panel) up to the event itself (e.g. March 1997) at the top.

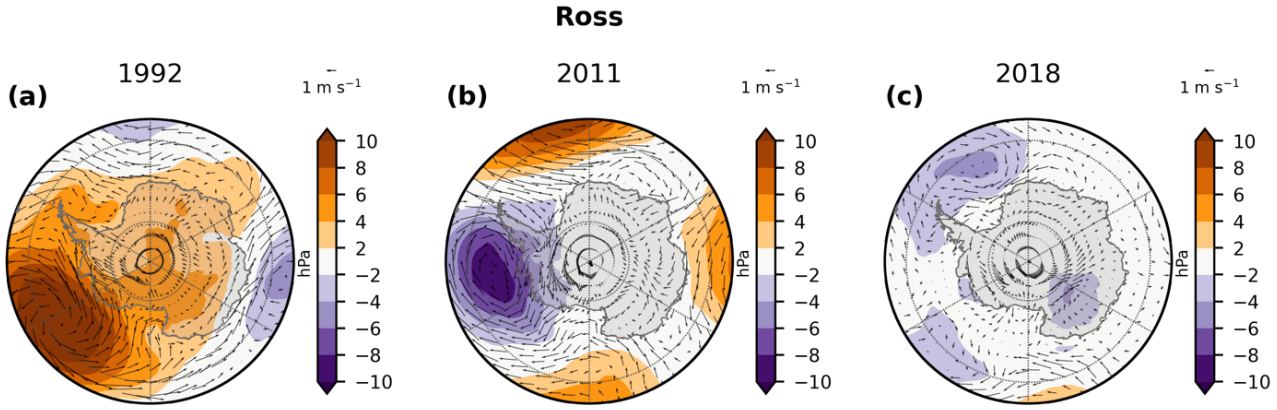

Figure S10: SLP (shading) and 10-m wind (arrows) anomalies in the years with SIE minima in the Ross Sea during the previous spring (OND).

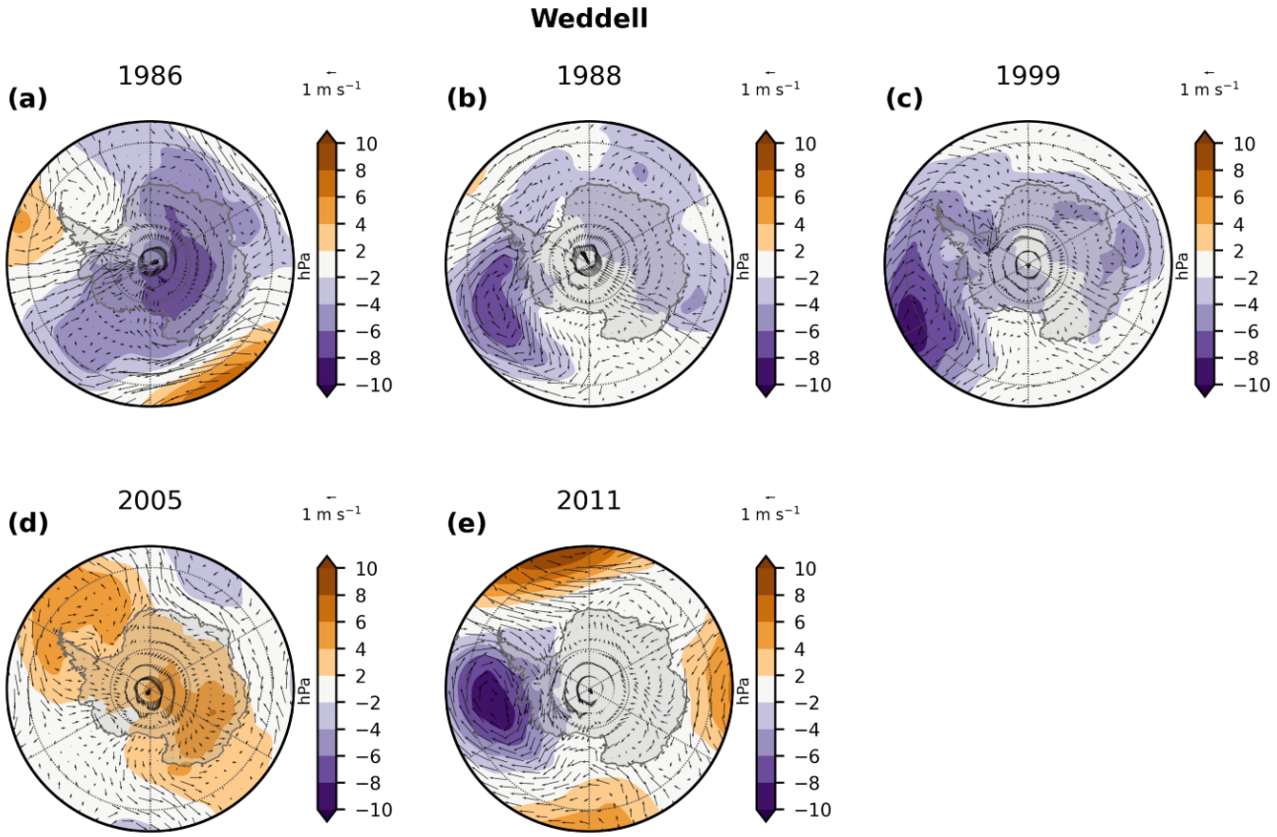

Figure S11: SLP (shading) and 10-m wind (arrows) anomalies in the years with SIE minima in the Weddell Sea during the previous spring (OND).

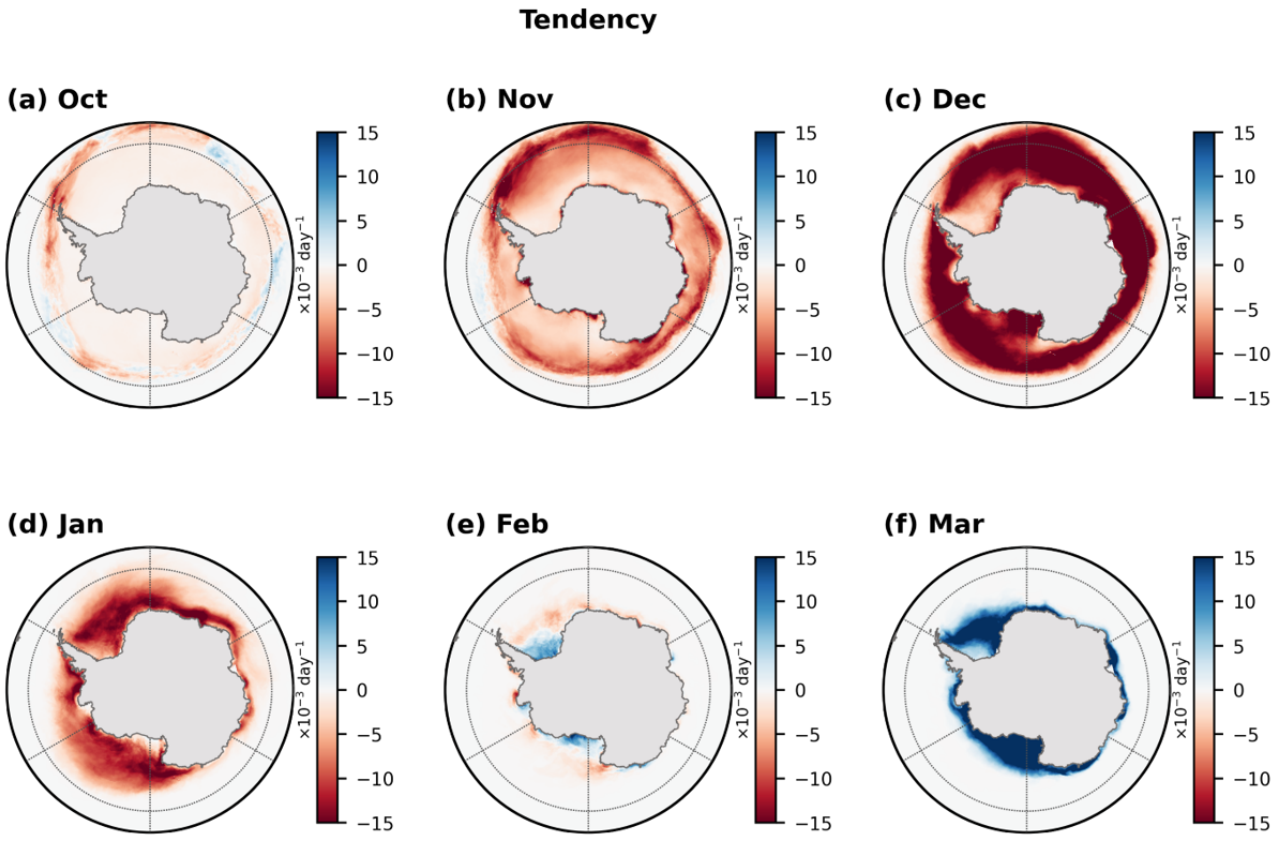

Figure S12: Monthly climatology of the late spring and summer tendency term of the model's SIC budget.

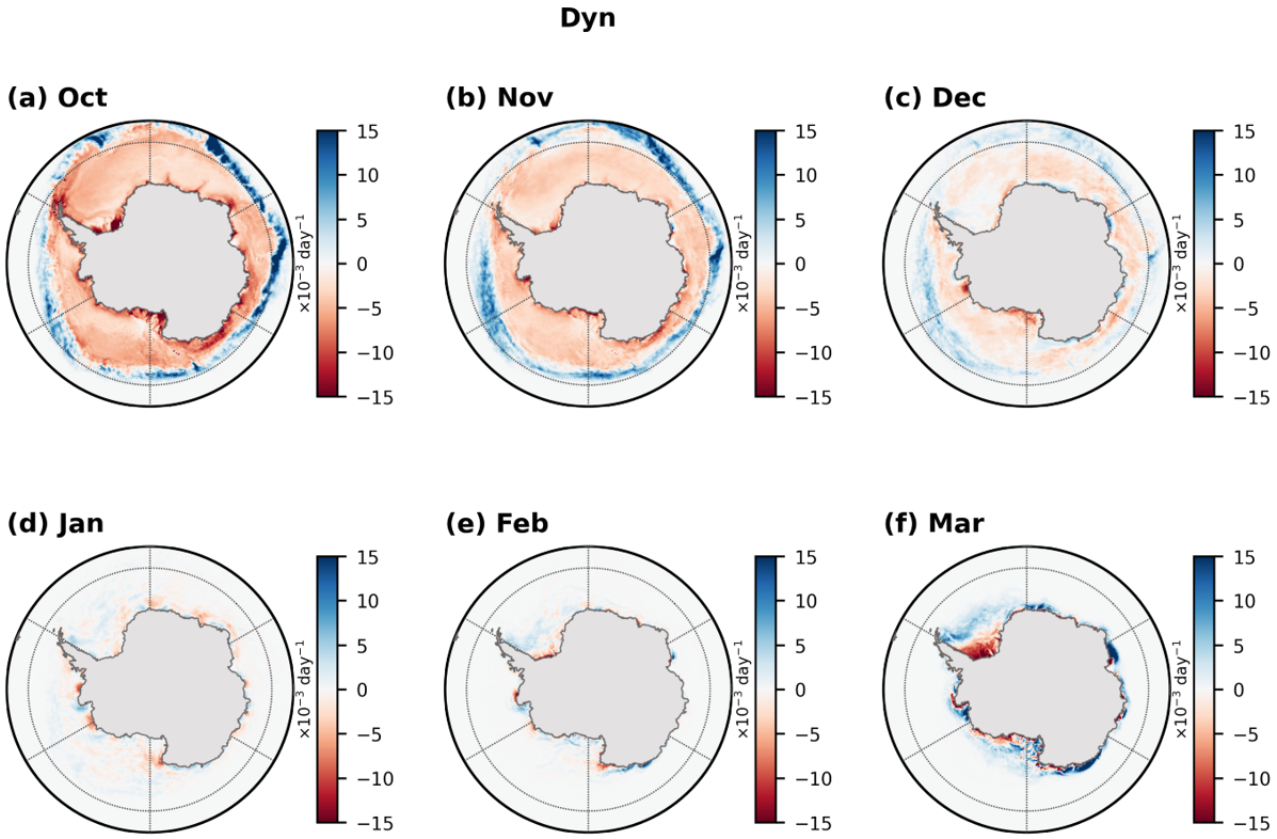

Figure S13: Monthly climatology of the late spring and summer dynamic term of the model's SIC budget.

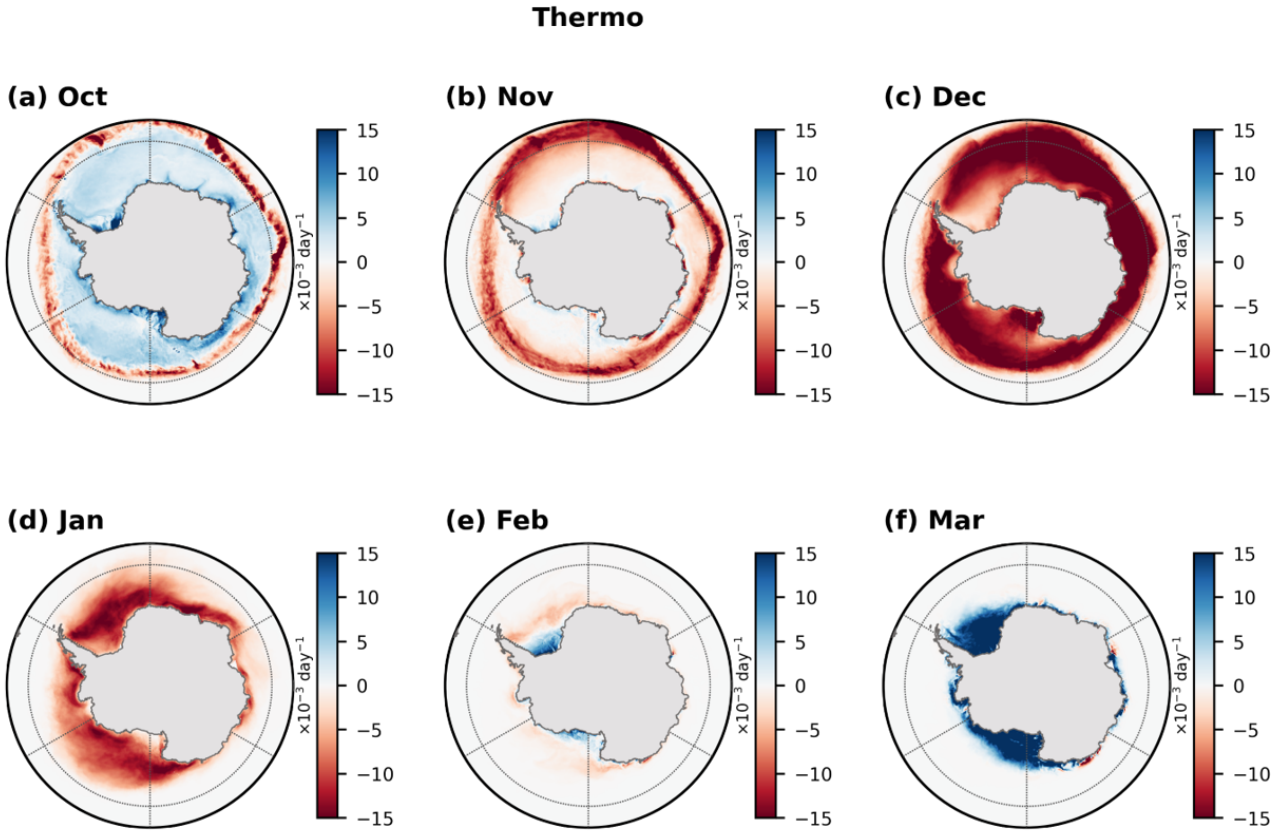

Figure S14: Monthly climatology of the late spring and summer thermodynamic term of the model's SIC budget.

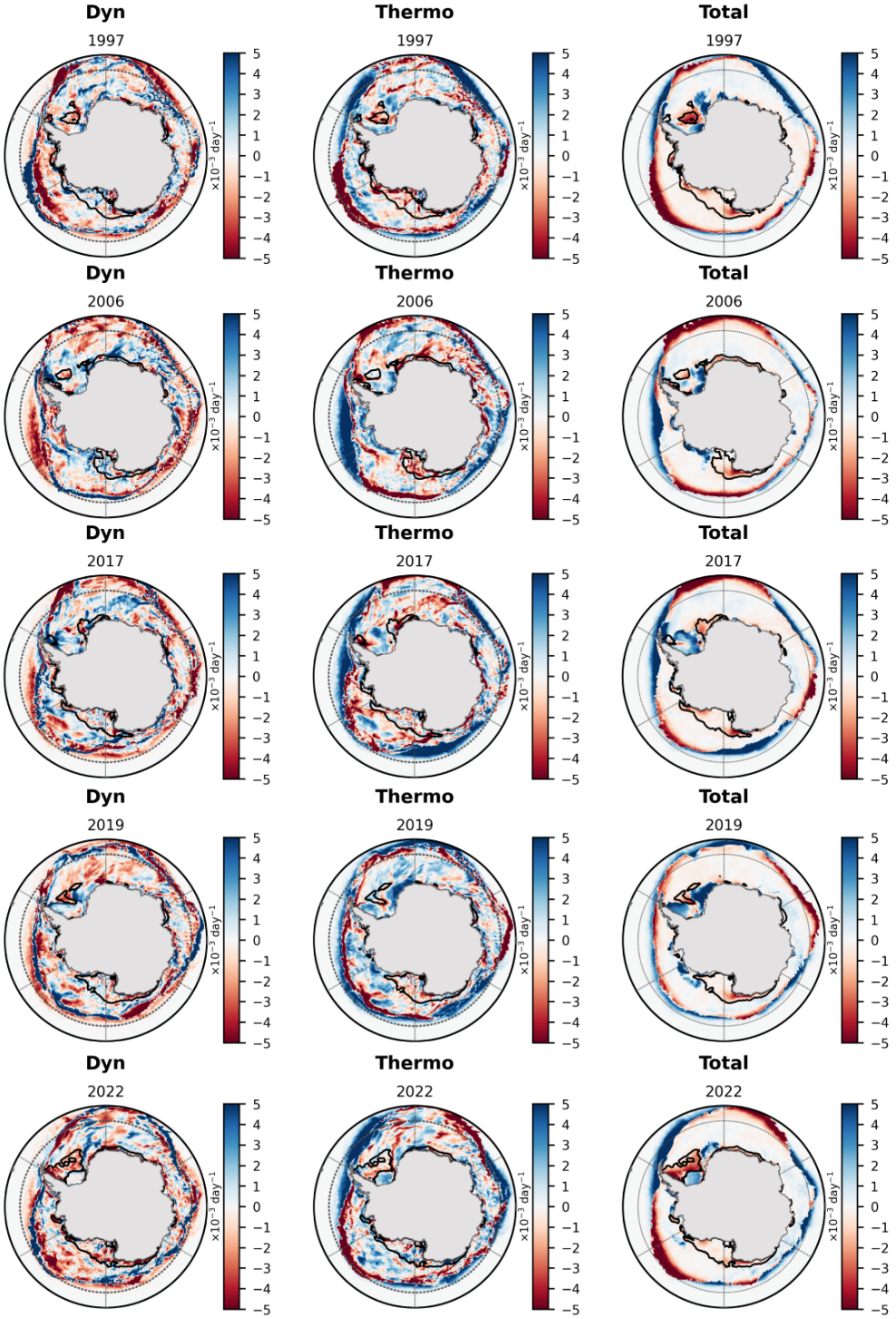

Figure S15: Shading: NDJ anomalies of the dynamic (left), thermodynamic (middle) and tendency (right) terms in the years with total SIE minima. Contours: areas with anomalous SIC = 0.1 in the corresponding year in JFM.

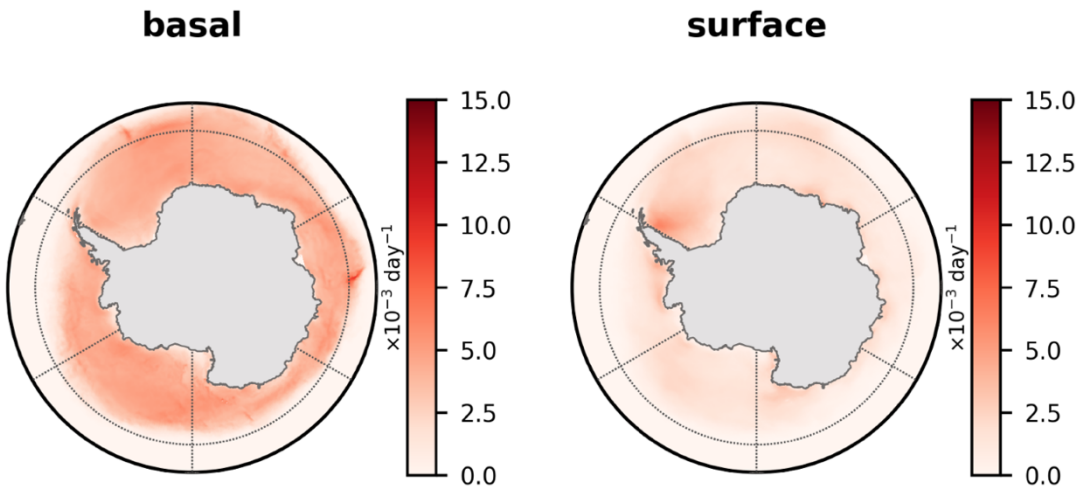

Figure S16: NDJ climatologies of the basal (left) and surface (right) melt components in the model.

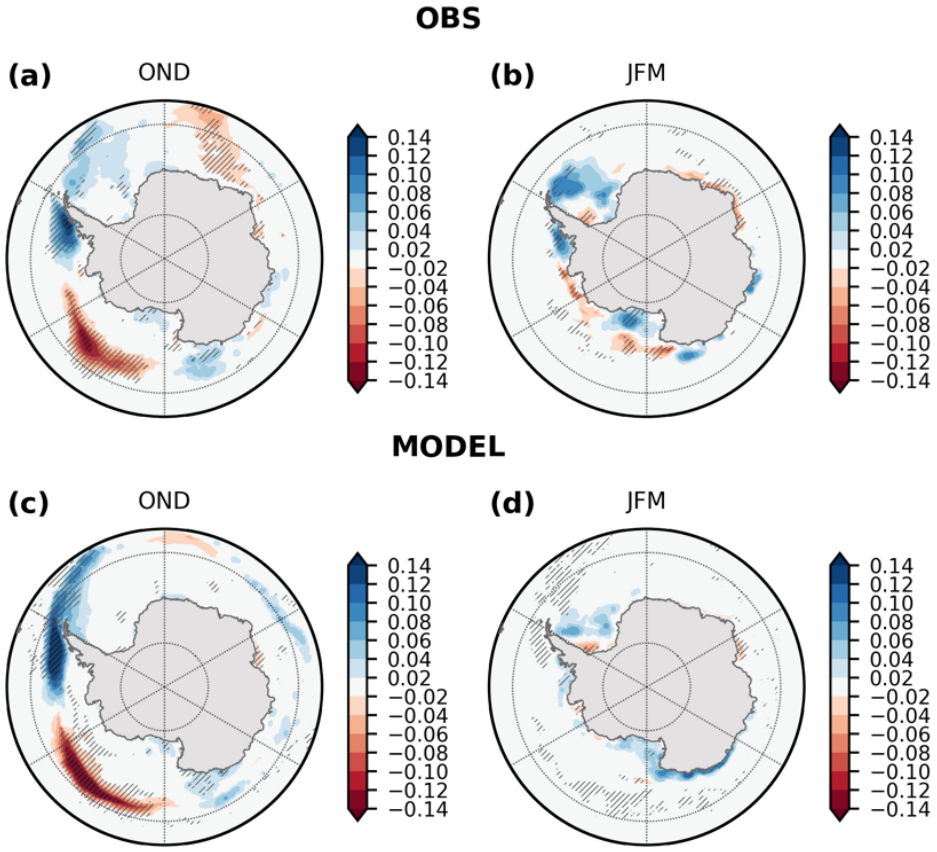

Figure S17: Linear regression of SIC anomalies on the DFJ Niño3.4 index in spring (left) and summer (right), representing the linear response to the warm ENSO phase (El Niño). Top: observations. Bottom: model. The Niño3.4-index is computed as the standardized area-averaged SST anomalies from HadISST over the Niño3.4 region (5°S–5°N, 170°–120°W). Hatches indicate statistical significance.

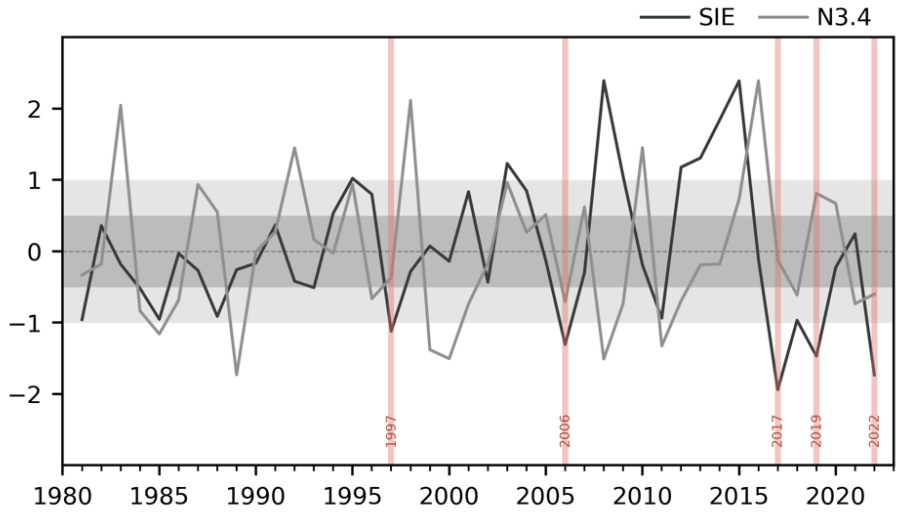

Figure S18: Black line: standardized SIE anomalies in JFM computed over the total SO domain in the observations. Grey line: DJF Niño3.4-index. Dark and light grey shadings indicate the ±0.5 and ±1σ, respectively. Years with a minimum SIE are marked in red.

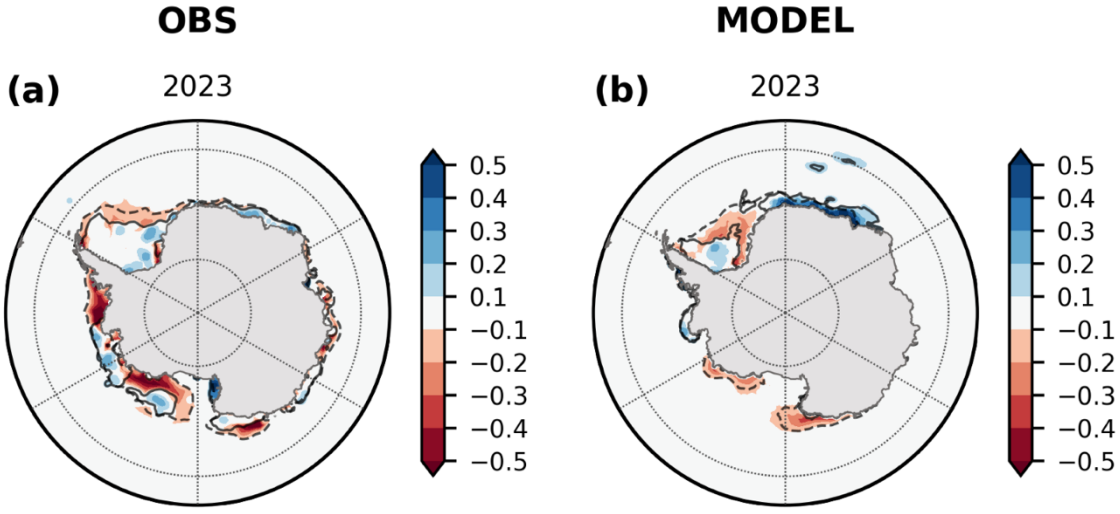

Figure S19: Shading: observed (left) and modelled (right) SIC anomalies in JF 2023 (March is excluded due to data unavailability). Contours: sea ice edge (SIC=0.15) in 2023 (solid line) and in the climatology (dashed line).

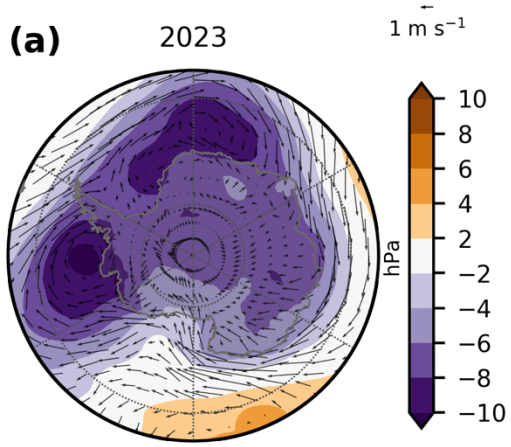

Figure S20: SLP (shading) and 10-m wind (arrows) anomalies in OND 2022, before the 2023 summer minimum.